Stabilizer Quantum Error Correction Toolbox for Superconducting Qubits

Simon E. Nigg and S. M. Girvin

Phys. Rev. Lett. **110**, 243604 — Published 14 June 2013

DOI: 10.1103/PhysRevLett.110.243604

Stabilizer quantum error correction toolbox for superconducting qubits

Simon E. Nigg and S. M. Girvin
Department of Physics, Yale University, New Haven, CT 06520, USA
(Dated: May 1, 2013)

We present a general protocol for stabilizer operator measurements in a system of N superconducting qubits. Using the dispersive coupling between the qubits and the field of a resonator as well as single qubit rotations, we show how to encode the parity of an arbitrary subset of $M \leq N$ qubits, onto two quasi-orthogonal coherent states of the resonator. Together with a fast cavity readout, this enables the efficient measurement of arbitrary stabilizer operators without locality constraints.

PACS numbers: 42.50.Ct,85.25.Am,42.50.Pq,03.67.-a

Several milestones on the road to quantum computing with superconducting circuits have recently been reached, such as the experimental violation of Bell's inequality [1] and the demonstration of rudimentary quantum error correction (QEC) [2]. As the resources required for more complete QEC protocols come within experimental reach, it is desirable to develop a toolbox sufficiently versatile to allow the implementation of a wide class of codes. Most QEC codes can be described concisely in the stabilizer formalism of Gottesman [3]. In this framework a QEC code is defined by the subspace spanned by the eigenstates with eigenvalue $+1$ of a set of commuting multi-qubit Pauli operators called stabilizer operators. Error detection is achieved by measuring the stabilizer operators of the code; the syndrome of an error being a sign flip of a subset of these operators. Correction in turn, can be performed when the syndrome contains enough information to identify the location and type of the error. The ability to measure arbitrary multi-qubit Pauli operators would thus allow a direct realization of stabilizer QEC codes, including non-local quantum low density parity check codes [4].

Toric and surface codes [5, 6] defined on two-dimensional qubit lattices are promising stabilizer codes with high thresholds for fault-tolerance [7]. However because the elementary (anyonic) excitations of these systems can diffuse at no energy cost, quantum memories built from these codes are thermally unstable [8, 9]. Thermal stability can be obtained by engineering effective interactions between the anyons [10, 11] or by going to four dimensions, where deconfinement of anyons is energetically suppressed [12]. To be physically realizable however, the latter needs to be mapped back onto a lattice of qubits with dimension $D \leq 3$. This mapping inevitably leads to *non-local* stabilizer operators, which one must be able to measure. In this work we take a first step in this direction and propose a scheme to measure arbitrary stabilizer operators in a system of superconducting qubits off-resonantly coupled to a common mode of a microwave resonator.

Several schemes for parity measurements of superconducting qubits have recently been proposed [13–15]. The main advantage of our approach is the ability to *selectively address an arbitrary subset of qubits*, without the need for tunable couplings, in contrast to earlier work [16, 17], and without restrictions on the number of and distance between physical qubits defining a given stabilizer operator. We thus extend the superconducting qubit toolbox with functionality similar to that recently demonstrated for trapped ions [18].

Central to our proposal is the off-resonant coupling between a superconducting qubit and a single mode of a microwave resonator [19] described by the dispersive Hamiltonian $H_{\rm disp} = \chi \boldsymbol{\sigma}^z \boldsymbol{a}^\dagger \boldsymbol{a}$, where $\boldsymbol{\sigma}^z = |e\rangle\langle e| - |g\rangle\langle g|$ is the Pauli matrix in the computational basis $\{|g\rangle, |e\rangle\}$ of the qubit and $\boldsymbol{a}$ ($\boldsymbol{a}^\dagger$) denotes the photon annihilation (creation) operator of the cavity mode. This coupling describes a qubit-state-dependent frequency shift $\pm\chi$ of the cavity, or equivalently a photon-number-dependent frequency shift $2n\chi$ of the qubit. In the weakly dispersive regime $2\chi \sim 1/T_2, \kappa$, where κ is the bare cavity linewidth and $T_2^{-1} = (2T_1)^{-1} + \Gamma_\phi$ is the qubit coherence time composed of relaxation $1/T_1$ and pure dephasing Γ_ϕ, this interaction enables a qubit-readout by measuring the phase-shift of transmitted or reflected microwaves [19]. In this work, we are interested in the ultrastrong dispersive regime of well-resolved resonances [20], where $\kappa, T_2^{-1} \ll \chi$. In this regime, we show how to encode the two eigenvalues of an arbitrary multi-qubit Pauli operator onto quasi-classical oscillations of light that differ in phase by π.

Although our scheme is applicable to other types of superconducting qubits, for clarity we will frame our discussion around the specific case of transmon qubits. A transmon qubit [21, 22] is formed by a superconducting dipole-antenna with a Josephson junction at its center with Josephson energy $E_J \gg E_C \equiv e^2/(2C_\Sigma)$, where C_Σ represents the total capacitance between the antenna pads. Neglecting charge-dispersion effects, which are suppressed exponentially in E_J/E_C [21], the low-energy spectrum of an isolated transmon is well approximated by that of an anharmonic oscillator with frequency $\omega_{01} \approx \sqrt{8E_J E_C} - E_C$ and weak anharmonicity $\omega_{01} - \omega_{12} \approx E_C \ll \omega_{01}$. In state-of-the-art realizations, the qubit linewidth $1/T_2$ is close to being limited by relaxation [22–25]. In this work we are interested in a setup

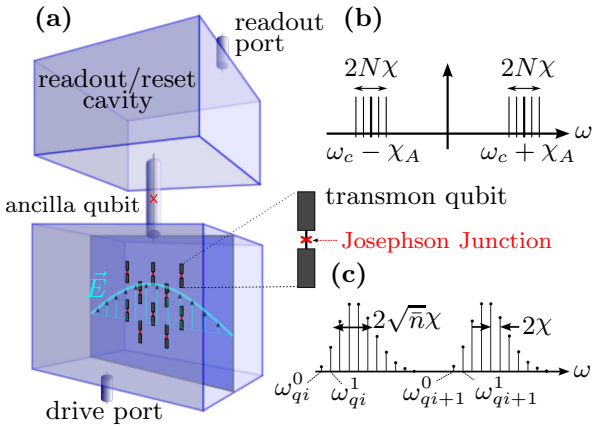

FIG. 1. (Color online) **(a)** 2D array of N transmon qubits in a 3D cavity. The ancilla qubit and the upper cavity are used for readout/reset and manipulation purposes. Cavity **(b)** and qubit **(c)** spectra in the ultra-strong dispersive regime.

such as depicted in Fig. 1 (a), where N transmons are coupled dispersively with strength χ to a microwave field inside a 3D cavity. For simplicity, we here discuss the case of equal dispersive couplings. In the supplemental material we show how to cope with the more realistic case of unequal dispersive shifts. For control and readout purposes, an ancilla qubit, is further dispersively coupled to both the high-Q cavity containing the N qubits with $\chi_A \gg N\chi$ and to a low-Q (readout) cavity, similar to the setup used in [26]. We assume that both the ancilla qubit and the readout cavity remain in the ground state, except during readout and manipulation. Thus omitting, for now, the corresponding degrees of freedom, we model this system in an appropriately rotating frame (see supplemental material for details), by the effective Hamiltonian

$$H_0 = \chi \sum_{i=1}^{N} \boldsymbol{\sigma}_i^z \boldsymbol{a}^\dagger \boldsymbol{a} - K \boldsymbol{a}^\dagger \boldsymbol{a}^\dagger \boldsymbol{a} \boldsymbol{a} \,. \tag{1}$$

The transmons are treated here as two-level systems assuming their anharmonicity is larger than their linewidth (i.e. $E_C > 1/T_2$). Furthermore, assuming the qubits to be sufficiently detuned from each other, we neglect the cavity-mediated qubit-qubit interaction. The latter leads to frequency shifts of the order of χ^2/Δ, where Δ is the detuning between the two qubits. For the parameters used below ($\chi = 5\,\mathrm{MHz}$ and $\Delta \geq 2\,\mathrm{GHz}$), these shifts are smaller than about 10 KHz. The second term on the rhs of Eq. (1) accounts for the (negative) qubit-induced anharmonicity of the cavity [27, 28]. In the weak dispersive regime, this term can usually be neglected as $K \ll \chi$. We find that in the ultra-strong dispersive regime it is necessary to account for its leading order effect. We next show how to encode the parity $\boldsymbol{Z}_{S_N} = \bigotimes_{i=1}^{N} \boldsymbol{\sigma}_i^z$ of an N-qubit state $|\psi\rangle_N$ onto two quasi-orthogonal coherent states of the cavity differing in phase by π.

Parity encoding. Suppose the system is initially prepared in the product state $|\Psi\rangle_{t=0} = |\alpha\rangle\,|\psi\rangle_N$, where $|\alpha\rangle$ is a coherent state of the cavity with amplitude α. Making use of the identity $\exp[-i(\pi/2)\sum_{i=1}^{N}\boldsymbol{\sigma}_i^z] = (-i)^N \boldsymbol{Z}_{S_N}$, one can show that under the action of (1), at time $T = \pi/(2\chi)$, the state becomes

$$|\Psi\rangle_T = \boldsymbol{U}_K \left(|\alpha_N\rangle\, \boldsymbol{P}^+_{S_N} + |-\alpha_N\rangle\, \boldsymbol{P}^-_{S_N} \right) |\psi\rangle_N \,, \tag{2}$$

where $\boldsymbol{P}^\pm_{S_N} = (\mathbb{1} \pm \boldsymbol{Z}_{S_N})/2$ are the projectors onto the even (+) and odd (−) qubit parity subspaces as measured by the ± 1 eigenvalues of the multi-qubit Pauli operator $\boldsymbol{Z}_{S_N}$ and $\alpha_N = (-i)^N \alpha$. Note that the self-Kerr term is qubit-independent [29] and conserves the photon number $\boldsymbol{a}^\dagger \boldsymbol{a}$. Because it commutes with the dispersive term, its effect factors out and is captured in (2) by the unitary operator $\boldsymbol{U}_K = \exp[i\pi K/(2\chi) \boldsymbol{a}^\dagger \boldsymbol{a}^\dagger \boldsymbol{a}\boldsymbol{a}]$. For weak nonlinearity such that $\pi K \ll \chi$, the leading order effect of $\boldsymbol{U}_K$ acting on the coherent states $|\pm\alpha_N\rangle$ is a rotation of the mean amplitude by an angle $\Delta\phi_{\mathrm{nl}} = \pi \bar{n} K/\chi$ with the mean photon number $\bar{n} = |\alpha|^2$. To leading order in K/χ, the state (2) is thus well approximated by

$$|\Psi\rangle_T = |\tilde{\alpha}_N\rangle\, \boldsymbol{P}^+_{S_N} |\psi\rangle_N + |-\tilde{\alpha}_N\rangle\, \boldsymbol{P}^-_{S_N} |\psi\rangle_N \,, \tag{3}$$

with $\tilde{\alpha}_N = \alpha_N e^{-i\Delta\phi_{\mathrm{nl}}}$. The sub-leading order effect is a damping of the mean amplitude by a factor $\exp(-\Delta\phi_{\mathrm{nl}}^2/(2\bar{n}))$ [30]. We emphasize that in the ultra-strong dispersive regime $\kappa/\chi \ll 1$ considered here, photon decay only weakly damps the amplitude of the coherent states in (3) by a factor $\exp(-\kappa T/2) \approx 1 - (\pi/4)(\kappa/\chi)$. Ignoring these small effects, we thus see that the dispersive interaction can be used to encode the parity of the multi-qubit state onto two coherent states of the cavity differing in phase by π.

Subset selectivity. Typically stabilizer operators are defined on subsets of qubits. Selectivity to $M \leq N$ qubits, labeled by the set $S_M \subseteq S_N = \{1, \ldots, N\}$, can be achieved as follows. Consider the identity

$$\boldsymbol{U}_{S_M}(t) = \Big(\bigotimes_{i \notin S_M} \boldsymbol{\sigma}_i^x \Big) \boldsymbol{U}_{S_N}\Big(\frac{t}{2}\Big) \Big(\bigotimes_{i \notin S_M} \boldsymbol{\sigma}_i^x \Big) \boldsymbol{U}_{S_N}\Big(\frac{t}{2}\Big), \tag{4}$$

where $\boldsymbol{U}_S(t) = \exp(-it\chi \boldsymbol{a}^\dagger \boldsymbol{a} \sum_{i\in S} \boldsymbol{\sigma}_i^z)$. Eq. (4) can be easily shown using $\boldsymbol{\sigma}^x \boldsymbol{\sigma}^z \boldsymbol{\sigma}^x = -\boldsymbol{\sigma}^z$. Thus, by splitting the dispersive evolution of all N qubits into two equal halves and interspersing them with bit-flip operations on the qubits not in S_M, we can effectively echo away the contribution of the latter to the total "magnetization" and implement the dispersive evolution $\boldsymbol{U}_{S_M}(t)$ of the qubits in S_M alone. Acting on an initial state of the form $|\alpha\rangle\,|\psi\rangle_N$, $\boldsymbol{U}_{S_M}(T = \pi/(2\chi))$ then encodes the subset-parity $\boldsymbol{Z}_{S_M} = \bigotimes_{i\in S_M} \boldsymbol{\sigma}_i^z$ onto the state of the cavity as explained above. The case of unequal dispersive shifts is treated in the supplemental material.

Physically, the initial unconditional cavity displacement and bit-flips can be implemented via fast microwave pulses (see supplemental material). Because

of the dispersive interaction, the qubit transition frequency of the i-th qubit splits into a ladder of frequencies $\omega_{qi}^n = \omega_{qi}^0 + 2n\chi$, corresponding to different photon numbers in the cavity (Fig. 1 (c)). The latter are Poisson distributed and peaked around $\bar{n}$. Hence, to best approximate an unconditional rotation of the i-th qubit, the pulse must be centered at the frequency $\omega_{qi}^0 + 2\bar{n}\chi$ and have a frequency-width large compared with $2\sqrt{\bar{n}}\,\chi$. For $|\alpha| \geq 1/\pi$ the duration of such a π-pulse is thus $T_\pi \ll 1/(2\sqrt{\bar{n}}\chi) \leq T$. Similarly, the initial coherent state of the cavity $|\alpha\rangle$ can be prepared from the vacuum by driving the cavity at the frequency $\omega_c - \chi_A$ with a pulse of area α and a frequency-width large compared with $2N\chi$; the maximal frequency spread of a cavity dispersively coupled with strength χ to N qubits (Fig. 1 (b)). Again the duration T_d of this pulse is short since $T_d \ll 1/(2N\chi) < T$. The total duration of the encoding is thus dominated by the dispersive evolution time $T = \pi/(2\chi)$, which is independent of N and M.

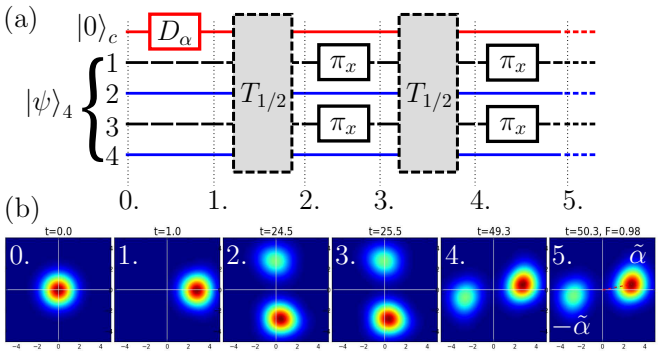

FIG. 2. (Color online) **(a)** Quantum circuit diagram for encoding the parity of qubits 2 and 4 (full (blue) lines). D_α represents the displacement operation, π_x a single-qubit π-pulse and $T_{1/2}$ a free dispersive evolution of duration $\pi/(4\chi)$. **(b)** Numerical simulation of the evolution of the Q-function of the cavity [30], with an initial qubit state $|\psi\rangle_4 = (|ggge\rangle + |ggeg\rangle + |eeeg\rangle)/\sqrt{3}$. Dissipation from photon loss at a rate $\kappa/(2\pi) = 10\,\mathrm{KHz}$ and qubit decoherence with $T_1 = T_2 = 20\,\mu\mathrm{s}$ are included as well as a finite displacement and π-pulse duration of 1 ns. Other parameters are: $\alpha = 2$, $\chi/(2\pi) = 5\,\mathrm{MHz}$ and $K/(2\pi) = 80\,\mathrm{KHz}$. The self-Kerr term leads to an additional phase rotation $\Delta\phi_{\mathrm{nl}} = 2K\bar{n}\Delta t$, where $\Delta t = 50.3\,\mathrm{ns}$ is the total duration of the encoding. Taking this rotation into account, we obtain a fidelity of $F = 98\%$ to the ideal target state $|\Psi\rangle_{\mathrm{ideal}} = |\tilde{\alpha}_2\rangle\, \boldsymbol{P}^+_{\{2,4\}}\, |\psi\rangle_4 + |-\tilde{\alpha}_2\rangle\, \boldsymbol{P}^-_{\{2,4\}}\, |\psi\rangle_4$.

As an example, Fig. 2 shows the results of a numerical simulation encoding the parity of $M = 2$ out of $N = 4$ qubits, which accounts for finite (square) pulse duration, decoherence and qubit-induced cavity nonlinearity. For the parameter values given in the caption, we find a fidelity (overlap with the ideal target state) of 98%. By applying single-qubit rotations to individual qubits before and after the encoding one may similarly encode the parity of an arbitrary weight M Pauli operator $\boldsymbol{Q}_{S_M} = \bigotimes_{i\in S_M} \boldsymbol{\tau}_i$, with $\boldsymbol{\tau}_i \in \{\boldsymbol{\sigma}_i^x, \boldsymbol{\sigma}_i^y, \boldsymbol{\sigma}_i^z\}$.

Parity readout. The encoded state is of the form $|\Psi\rangle_T = |\tilde{\alpha}_M\rangle\, \boldsymbol{P}^+_{S_M}\, |\psi\rangle_N + |-\tilde{\alpha}_M\rangle\, \boldsymbol{P}^-_{S_M}\, |\psi\rangle_N$, where $\boldsymbol{P}^\pm_{S_M} = (\mathbb{1} \pm \boldsymbol{Q}_{S_M})/2$ and $\tilde{\alpha}_M = (-i)^M e^{-i\Delta\phi_{\mathrm{nl}}}\alpha$. The overlap between the two cavity states, $\langle\tilde{\alpha}_M|-\tilde{\alpha}_M\rangle = \exp(-2|\alpha|^2)$, is independent of K and M. For large $|\alpha|$, these two states are distinguishable in principle and a measurement of the cavity state is equivalent to a multi-qubit parity measurement. A fast readout of the cavity state with $T_{\mathrm{meas}} \ll 1/\kappa$, may be achieved by lowering the Q-factor of the cavity containing the qubits ($\kappa \to \kappa' \gg \kappa$), as recently demonstrated [31]. This Q-switching adversely affects the lifetime of the qubits via the Purcell effect. However, the latter is expected to be weak as long as $\kappa' \ll \chi$. Alternatively, the cavity state can be mapped onto the ancilla qubit, which can subsequently be measured through standard homodyne measurement of the low-Q readout cavity. The mapping is achieved physically in three steps. First, the high-Q cavity field is displaced unconditionally by $\tilde{\alpha}_M$. To a good approximation, this maps the encoded state onto

$$\boldsymbol{D}_{\tilde{\alpha}_M}\, |\Psi\rangle_T = |2\tilde{\alpha}_M\rangle\, \boldsymbol{P}^+_{S_M}\, |\psi\rangle_N + |0\rangle\, \boldsymbol{P}^-_{S_M}\, |\psi\rangle_N\,. \qquad (5)$$

The second step consists in performing a π-pulse on the ancilla qubit, which so far was in its ground state, conditioned on the cavity being in the vacuum state. As first proposed in [32] and demonstrated in [26], this can be achieved by applying a pulse centered on the bare ancilla qubit transition frequency, which is narrow in frequency compared with $8\bar{n}\chi_A$ (the additional factor of 4 is due to the twice as large amplitude of the cavity state in the first term on the rhs of Eq. (5)). Because $\chi_A \gg N\chi$, a pulse duration T_A can be chosen such that $1/(2\chi_A) \ll T_A \ll 1/(2N\chi)$. For $\bar{n} > 1/4$ the first inequality guarantees conditionality while the second one allows us to neglect the dispersive evolution during this operation. The state then becomes approximately

$$|2\tilde{\alpha}_M\rangle \left(\boldsymbol{P}^+_{S_M}\, |\psi\rangle_N\right) |g\rangle_A + |0\rangle \left(\boldsymbol{P}^-_{S_M}\, |\psi\rangle_N\right) |e\rangle_A\,. \qquad (6)$$

In the third and final step, a displacement of $-2\tilde{\alpha}_M$ is performed on the cavity conditioned on the ancilla qubit being in the ground state. This is achieved with a pulse centered at frequency $\omega_c - \chi_A$, with a frequency-width small compared with $2\chi_A$ but large compared with $2N\chi$. Neglecting again the dispersive evolution during this step, the state finally becomes

$$|0\rangle \left[\left(\boldsymbol{P}^+_{S_M}\, |\psi\rangle_N\right) |g\rangle_A + \left(\boldsymbol{P}^-_{S_M}\, |\psi\rangle_N\right) |e\rangle_A\right]. \qquad (7)$$

Note that the state (7) is now stationary with respect to the dispersive interaction, there being no photons in the cavity. Reading out the state of the ancilla qubit amounts to measuring $\boldsymbol{Q}_{S_M}$. After the measurement, the ancilla qubit may be reset to the ground state efficiently via the readout cavity [33].

Simulated time evolution. The ancilla qubit can also be used to simulate the "time evolution" $\exp[-i\theta \boldsymbol{Q}_{S_M}]$ under the action of an arbitrary Pauli operator $\boldsymbol{Q}_{S_M}$. This is useful e.g. for manipulating a logical qubit state encoded in a stabilizer subspace in which case $\boldsymbol{Q}_{S_M}$ is taken to be a logical qubit Pauli operator. Starting from the state Eq. (5), this is achieved by adiabatically driving the ancilla around a closed loop on its Bloch sphere subtending a solid angle 4θ, conditioned on there being no photons in the cavity. The component in Eq. (5) with zero photons then acquires a phase of 2θ (half the solid angle) and the state becomes

$$|2\tilde{\alpha}_M\rangle \boldsymbol{P}^+_{S_M} |\psi\rangle_N + e^{2i\theta} |0\rangle \boldsymbol{P}^-_{S_M} |\psi\rangle_N . \qquad (8)$$

Note that $\chi_A \gg N\chi$ guarantees that the adiabatic condition wrt χ_A can be satisfied while still remaining fast wrt the dispersive time scale $1/(N\chi)$. In (8) we omitted the state of the ancilla qubit, since it starts and ends in the ground state and thus factors out. The cavity is disentangled from the state by applying the encoding protocol with α replaced by $-\tilde{\alpha}_M$. After unconditionally displacing the cavity back to the vacuum, taking into account an additional nonlinear phase acquired during the decoding, the N-qubit state finally becomes

$$\boldsymbol{P}^+_{S_M} |\psi\rangle_N + e^{2i\theta} \boldsymbol{P}^-_{S_M} |\psi\rangle_N = e^{i\theta} e^{-i\theta \boldsymbol{Q}_{S_M}} |\psi\rangle_N , \qquad (9)$$

which up to an unimportant global phase factor, represents the action of the desired unitary.

Application. To test the feasibility of the above protocols, we simulated the preparation of a logical qubit state of the four-qubit erasure channel code [34]. The stabilizer generators of this code are $S = \{Z_1Z_2, Z_3Z_4, X_1X_2X_3X_4\}$, where we have switched to the standard notation X_i and Z_i for the Pauli operators of qubit i. The code-space is spanned by the two $+1$ eigenstates of the stabilizer operators:

$$|\pm\rangle = \frac{1}{2}(|gg\rangle \pm |ee\rangle)(|gg\rangle \pm |ee\rangle). \qquad (10)$$

The logical qubit Pauli operators are $\overline{Z} = X_1X_2 = X_3X_4$ and $\overline{X} = Z_1Z_3 = Z_2Z_4 = Z_1Z_4 = Z_2Z_3$. Because of the redundancy of the logical operators, this code protects a logical qubit state $\alpha|+\rangle + \beta|-\rangle$ from the loss (i.e. arbitrary error) of a *known* qubit [34]. Here we prepare the logical qubit state $|\overline{\psi}\rangle = \exp[-i(\pi/8)\overline{X}]\,|+\rangle$ as follows. (i) We start with the fully polarized four-qubit state $|gggg\rangle$, which is already a $+1$ eigenstate of the Z stabilizer operators. (ii) Using the encoding protocol, we measure the logical $\overline{Z}$ operator X_1X_2. If we obtain -1, we apply Z_1. (iii) We measure the operator X_3X_4. If we obtain -1 we apply Z_3. (iv) We reset the cavity to the vacuum. These four steps prepare the logical state $|+\rangle$. We next use the ancilla (with $\chi_A = 10N\chi$) to implement the rotation as described above with $\boldsymbol{Q}_{S_4} = \overline{X}$ and $\theta = \pi/8$. Fig. 3 shows the obtained fidelity to the ideal target state $\exp[-i(\pi/8)\overline{X}]\,|+\rangle$ as a function of χ and K in units of $\kappa/(2\pi) = 10\,\mathrm{KHz}$ and for $T_1 = T_2 = 20\,\mu s$. The total duration T of the state preparation is shown on the upper x-axis in units of $1/\kappa$. Focusing on the line $K = 0$, when χ is small T is large and dominated by the dispersive evolutions and the fidelity is limited by a combination of qubit decoherence, photon loss and faulty conditional ancilla rotation. The fidelity then increases with increasing χ, which reduces the preparation time T and hence the effects of decoherence and improves the fidelity of the conditional ancilla rotation. It reaches a maximum in a regime where both conditional and unconditional operations can be performed with high fidelity. A further increase in χ degrades the unconditional cavity displacement and qubit rotations (a 1 ns pulse corresponds to a width of $\sim$ 160 MHz) and the fidelity drops. The cavity nonlinearity K and the dispersive shift χ are in fact not independent, but rather related via the single-qubit anharmonicity α_q, by the inequality $K \geq \chi^2/(4\alpha_q)$ [27], which is shown as a dashed (red) curve in Fig. 3 for $\alpha_q/(2\pi) = 200\,\mathrm{MHz}$.

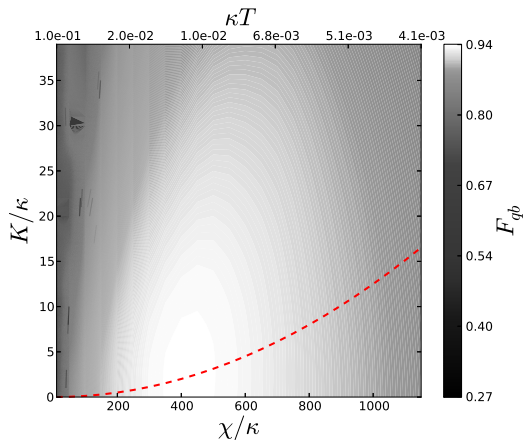

FIG. 3. (Color online) Fidelity of the prepared state to $\exp[-i(\pi/8)\overline{X}]\,|+\rangle$. The (red) dashed curve represents the boundary of the inequality $K \geq \chi^2/(4\alpha_q)$ which relates the self-Kerr K with the dispersive shift χ and the single-qubit anharmonicity α_q [27]. Here $\alpha_q/(2\pi) = 200\,\mathrm{MHz}$.

In conclusion, we proposed a protocol to measure stabilizer operators defined on an arbitrary subset of superconducting qubits in the ultra-strong dispersive regime of cQED. Challenges for the future will be to extend the present protocol to carry out multiple stabilizer measurements in parallel and to make it scalable perhaps by using multiple cavities as in [14] and an efficient encoding of multiple bits of information onto the photonic Hilbert space [32].

We thank L. Jiang, M. Mirrahimi, D. Poulin, M. Devoret and R. Schoelkopf for discussions. The simulations were coded in Python using the QuTip library [35]. This work was supported by the Swiss NSF, the NSF (DMR-

1004406) and the ARO (W911NF-09-1-0514).

[1] M. Ansmann, H. Wang, R. C. Bialczak, M. Hofheinz, E. Lucero, M. Neeley, A. D. O'Connell, D. Sank, M. Weides, J. Wenner, A. N. Cleland, and J. M. Martinis, Nature **461**, 504 (2009).

[2] M. D. Reed, L. DiCarlo, S. E. Nigg, L. Sun, L. Frunzio, S. M. Girvin, and R. J. Schoelkopf, Nature **482**, 382 (2012).

[3] D. Gottesman, *Stabilizer Codes and Quantum Error Correction*, Ph.D. thesis, Caltech (1997).

[4] D. J. C. MacKay, G. Mitchison, and P. L. McFadden, IEEE Transactions on Information Theory **50**, 2315 (2004); A. A. Kovalev and L. P. Pryadko, "Quantum "hyperbicycle" low-density parity check codes with finite rate," (2013), arXiv:quant-ph/1212.6703v2.

[5] A. Kitaev, Annals of Physics **303**, 2 (2003).

[6] S. Bravyi and A. Kitaev, "Quantum codes on a lattice with boundary," (1998), arXiv:quant-ph/9811052.

[7] D. S. Wang, A. G. Fowler, A. M. Stephens, and L. C. L. Hollenberg, Quantum Information & Computation **10**, 456 (2010); A. G. Fowler, M. Mariantoni, J. M. Martinis, and A. N. Cleland, Phys. Rev. A **86**, 032324 (2012).

[8] E. Dennis, A. Kitaev, A. Landahl, and J. Preskill, Journal of Mathematical Physics **43**, 4452 (2002).

[9] O. Landon-Cardinal and D. Poulin, Phys. Rev. Lett. **110**, 090502 (2013).

[10] S. Chesi, B. Röthlisberger, and D. Loss, Phys. Rev. A **82**, 022305 (2010).

[11] A. Hutter, J. R. Wootton, B. Röthlisberger, and D. Loss, Phys. Rev. A **86**, 052340 (2012).

[12] R. Alicki, M. Horodecki, P. Horodecki, and R. Horodecki, Open Systems & Information Dynamics **17**, 1 (2010).

[13] K. Lalumière, J. M. Gambetta, and A. Blais, Phys. Rev. A **81**, 040301 (2010).

[14] D. P. DiVincenzo and F. Solgun, (2012), arXiv:1205.1910 [quant-ph].

[15] T. Tanamoto, V. M. Stojanovic, C. Bruder, and D. Becker, (2013), arXiv:1301.4796 [quant-ph].

[16] T. P. Spiller, K. Nemoto, S. L. Braunstein, W. J. Munro, P. van Loock, and G. J. Milburn, New Journal of Physics **8**, 30 (2006).

[17] C. R. Myers, M. Silva, K. Nemoto, and W. J. Munro, Phys. Rev. A **76**, 012303 (2007).

[18] J. T. Barreiro, M. Müller, P. Schindler, D. Nigg, T. Monz, M. Chwalla, M. Hennrich, C. F. Roos, P. Zoller, and R. Blatt, Nature **470**, 486 (2011); M. Müller, K. Hammerer, Y. L. Zhou, C. F. Roos, and P. Zoller, New. J. Phys. **13**, 085007 (2011).

[19] A. Blais, R.-S. Huang, A. Wallraff, S. M. Girvin, and R. J. Schoelkopf, Phys. Rev. A **69**, 062320 (2004).

[20] D. I. Schuster, A. A. Houck, J. A. Schreier, A. Wallraff, J. M. Gambetta, A. Blais, L. Frunzio1, J. Majer, B. Johnson, M. H. Devoret, S. M. Girvin, and R. J. Schoelkopf, Nature **445**, 515 (2007).

[21] J. Koch, T. M. Yu, J. Gambetta, A. A. Houck, D. I. Schuster, J. Majer, A. Blais, M. H. Devoret, S. M. Girvin, and R. J. Schoelkopf, Phys. Rev. A **76**, 042319 (2007).

[22] H. Paik, D. I. Schuster, L. S. Bishop, G. Kirchmair, G. Catelani, A. P. Sears, B. R. Johnson, M. J. Reagor, L. Frunzio, L. I. Glazman, S. M. Girvin, M. H. Devoret, and R. J. Schoelkopf, Phys. Rev. Lett. **107**, 240501 (2011).

[23] M. Lenander, H. Wang, R. C. Bialczak, E. Lucero, M. Mariantoni, M. Neeley, A. D. O'Connell, D. Sank, M. Weides, J. Wenner, T. Yamamoto, Y. Yin, J. Zhao, A. N. Cleland, and J. M. Martinis, Phys. Rev. B **84**, 024501 (2011).

[24] G. Catelani, R. J. Schoelkopf, M. H. Devoret, and L. I. Glazman, Phys. Rev. B **84**, 064517 (2011).

[25] G. Catelani, S. E. Nigg, S. M. Girvin, R. J. Schoelkopf, and L. I. Glazman, Phys. Rev. B **86**, 184514 (2012).

[26] G. Kirchmair, B. Vlastakis, Z. Leghtas, S. E. Nigg, H. Paik, E. Ginossar, M. Mirrahimi, L. Frunzio, S. M. Girvin, and R. J. Schoelkopf, Nature **495**, 205 (2013).

[27] S. E. Nigg, H. Paik, B. Vlastakis, G. Kirchmair, S. Shankar, L. Frunzio, M. H. Devoret, R. J. Schoelkopf, and S. M. Girvin, Phys. Rev. Lett. **108**, 240502 (2012).

[28] J. Bourassa, F. Beaudoin, J. M. Gambetta, and A. Blais, Phys. Rev. A **86**, 013814 (2012).

[29] Qubit-state-dependent corrections to the self-Kerr are of order $\hat{\varphi}^6$ in an expansion of the Josephson potential $E_J \cos(\hat{\varphi})$ and are smaller by a factor $\sim \sqrt{E_C/E_J}$.

[30] D. F. Walls and G. J. Milburn, *Quantum optics*, 2nd ed. (Springer, 2008).

[31] Y. Yin, Y. Chen, D. Sank, P. J. J. O'Malley, T. C. White, R. Barends, J. Kelly, E. Lucero, M. Mariantoni, A. Megrant, C. Neill, A. Vainsencher, J. Wenner, A. N. Korotkov, A. N. Cleland, and J. M. Martinis, (2012), arXiv:1208.2950 [cond-mat].

[32] Z. Leghtas, G. Kirchmair, B. Vlastakis, M. H. Devoret, R. J. Schoelkopf, and M. Mirrahimi, Phys. Rev. A **87**, 042315 (2013).

[33] K. Geerlings, Z. Leghtas, I. M. Pop, S. Shankar, L. Frunzio, R. J. Schoelkopf, M. Mirrahimi, and M. H. Devoret, (2012), arXiv:1211.0491 [cond-mat.mes-hall].

[34] M. Grassl, T. Beth, and T. Pellizzari, Phys. Rev. A **56**, 33 (1997).

[35] J. Johansson, P. Nation, and F. Nori, Computer Physics Communications **183**, 1760 (2012).